

PAPER

# Experimental Investigation of Electronic Structure of $\text{La}(\text{O},\text{F})\text{BiSe}_2^*$

To cite this article: Jun Ma *et al* 2016 *Chinese Phys. Lett.* **33** 127401

View the [article online](#) for updates and enhancements.

## You may also like

- [Experimental overview on pairing mechanisms of  \$\text{BiCh}\_2\$ -based \(Ch: S, Se\) layered superconductors](#)  
Kazuhiisa Hoshi and Yoshikazu Mizuguchi
- [Bulk sensitive angle-resolved photoelectron spectroscopy on  \$\text{Nd}\(\text{O},\text{F}\)\text{BiS}\_2\$](#)   
K Terashima, J Sonoyama, M Sunagawa et al.
- [Investigation of in-plane anisotropy of  \$c\$ -axis magnetoresistance for  \$\text{BiCh}\_2\$ -based layered superconductor  \$\text{NdO}\_{0.7}\text{F}\_{0.3}\text{BiS}\_2\$](#)   
Kazuhiisa Hoshi, Kenta Sudo, Yosuke Goto et al.

## Experimental Investigation of Electronic Structure of La(O,F)BiSe<sub>2</sub> \*

Jun Ma(马俊)<sup>1</sup>, Bin-Bin Fu(付彬彬)<sup>1</sup>, Jun-Zhang Ma(马均章)<sup>1</sup>, Ling-Yuan Kong(孔令元)<sup>1</sup>, Di Chen(陈迪)<sup>1</sup>,  
 Ji-Feng Shao(邵继峰)<sup>3</sup>, Chang-Jin Zhang(张昌锦)<sup>3</sup>, Tian Qian(钱天)<sup>1,2</sup>,  
 Yu-Heng Zhang(张裕恒)<sup>3</sup>, Hong Ding(丁洪)<sup>1,2\*\*</sup>

<sup>1</sup>Beijing National Laboratory for Condensed Matter Physics, Institute of Physics, Chinese Academy of Sciences, Beijing 100190

<sup>2</sup>Collaborative Innovation Center of Quantum Matter, Beijing 100190

<sup>3</sup>High Magnetic field Laboratory of Chinese Academy of Sciences, University of Science and Technology of China, Hefei 230026

(Received 26 September 2016)

*La(O,F)BiSe<sub>2</sub> is a layered superconductor and has the same crystal structure with La(O,F)BiS<sub>2</sub>. We investigate the electronic structure of La(O,F)BiSe<sub>2</sub> using the angle-resolved photoemission spectroscopy. Two electron-like Fermi surfaces around  $X(\pi, 0)$  are observed, corresponding to the electron doping of 0.23 per Bi site. We clearly resolve anisotropic band splitting along both  $\Gamma-X$  and  $M-X$  due to the cooperative effects of large spin-orbit coupling and interlayer coupling. Moreover, we observe an almost non-dispersive electronic state around  $-0.2$  eV between the electron-like bands. This state vanishes after in-situ K evaporation, indicating that it could be the localized surface state caused by defects on the cleaved surface.*

PACS: 74.25.Jb, 74.70.-b, 71.18.+y, 71.20.-b

DOI: 10.1088/0256-307X/33/12/127401

Layered compounds have been intensively studied for the exploration of new high-transition-temperature superconductors, since the discovery of cuprate<sup>[1]</sup> and iron-based superconductors.<sup>[2]</sup> In 2013, superconductivity was initially reported in Bi<sub>4</sub>O<sub>4</sub>S<sub>3</sub>,<sup>[3–5]</sup> which is composed of the stacking of the superconducting BiS<sub>2</sub> layers and the blocking layers of Bi<sub>4</sub>O<sub>4</sub>(SO<sub>4</sub>)<sub>1–x</sub>. Subsequently, an analogous series of BiS<sub>2</sub>-based superconductors are discovered, including (Ln,Sr)O<sub>1–x</sub>F<sub>x</sub>Bi(S,Se)<sub>2</sub>,<sup>[6–13]</sup> where Ln denotes lanthanoid atoms.

As for the underlying mechanism of superconductivity related to this new series of superconductors, different theoretical scenarios have been proposed.<sup>[14–21]</sup> A two-orbital model<sup>[20]</sup> describes the band structure reasonably. Due to the low superconducting transition temperature and the weak correlation effect in *p* orbitals, electron-phonon coupling has been suggested to dominate the superconducting pairing.<sup>[16]</sup> This guess is consistent with the Raman scattering result<sup>[22]</sup> of this material, suggesting that the BiS<sub>2</sub>-based superconductors are possibly phonon-mediated BCS superconductors. However, another ARPES data<sup>[23]</sup> on NdO<sub>0.5</sub>F<sub>0.5</sub>BiS<sub>2</sub> was interpreted in terms of the presence of a polaronic state at the bottom of the electron-like bands near *X*, suggesting that the electron correlation effects play an important role in this material. Moreover, strong Fermi surface nesting at the wave vector  $(\pi, \pi)$  was predicted, which might enhance the electron-phonon interaction.<sup>[20]</sup> Among

numerous experiments, angle-resolved photoemission spectroscopy (ARPES) was used to investigate the Fermi surface and band dispersions of these materials. ARPES measurements<sup>[24,25]</sup> revealed a small band renormalization factor which indicates the rather weak electron correlation in this compound. One of the measurements indicated the Fermi surface nesting as predicted in this system, while the transition temperature was not enhanced. Moreover, neutron scattering work<sup>[26]</sup> and STM measurement<sup>[3,27]</sup> on this material gave contradictory results about the electron-phonon coupling strength. A *g*-wave pairing scenario was proposed at the low electron doping level, indicating an unconventional pairing symmetry.<sup>[21]</sup> Thus detailed experimental studies of the electronic structure is crucial in understanding this material.

In this Letter, we present ARPES results of the BiSe<sub>2</sub>-based superconductor La(O,F)BiSe<sub>2</sub> (*T<sub>c</sub>* = 3.7 K). We observed two discernible electron-like Fermi surfaces around the *X* point. The band splitting along the *M–X* direction was observed clearly for the first time. According to the Luttinger theorem, its carrier doping level is 0.23 electrons per Bi site. As a result, the measured electronic structure is far from the proposed FS nesting. Apparently, there is a discrepancy between the nominal and actual doping levels, which has been observed in other measurements.<sup>[25,27]</sup> The Bi deficiency was proposed to be the main reason. We performed EDS analysis on the sample, while the measurements on light elements (F/O) might have

\*Supported by the National Basic Research Program of China under Grant Nos 2015CB921300, 2013CB921700 and 2016YFA0300404, the National Natural Science Foundation of China under Grant Nos 11474340, 11234014, U1532267 and 11674327, and the Chinese Academy of Sciences under Grant No XDB07000000.

\*\*Corresponding author. Email: dingh@aphy.iphy.ac.cn

© 2016 Chinese Physical Society and IOP Publishing Ltd

large uncertainty. Thus we may have nonstoichiometry in this material. Furthermore, we observe an electronic state around 0.2 eV below  $E_F$  between the electron-like bands, which vanishes after the K evaporation. This indicates that this state could be the surface state caused by defects on the cleaved surface.

Large single crystal with a nominal composition of  $\text{LaO}_{0.3}\text{F}_{0.7}\text{BiSe}_2$  was synthesized by the flux method using a mixture of CsCl and KCl as the flux.<sup>[28]</sup> Energy dispersion spectrum (EDS) measurements were performed on several pieces of samples, which give an averaged composition of  $\text{LaO}_{0.54}\text{F}_{0.46}\text{Bi}_{0.99}\text{Se}_{1.93}$ . ARPES measurements were performed at the Dreamline beamline at the Shanghai Synchrotron Radiation Facility (SSRF), equipped with a Scienta D80 analyzer. The energy and angular resolutions of the ARPES measurements were set at 20 meV and  $0.1^\circ$ , respectively. The samples were cleaved *in situ* and measured at 22 K in a vacuum better than  $4 \times 10^{-11}$  Torr. The incident photon energy was chosen to be  $h\nu = 43$  eV. The K source used here for evaporation is made of a SAES K dispenser.

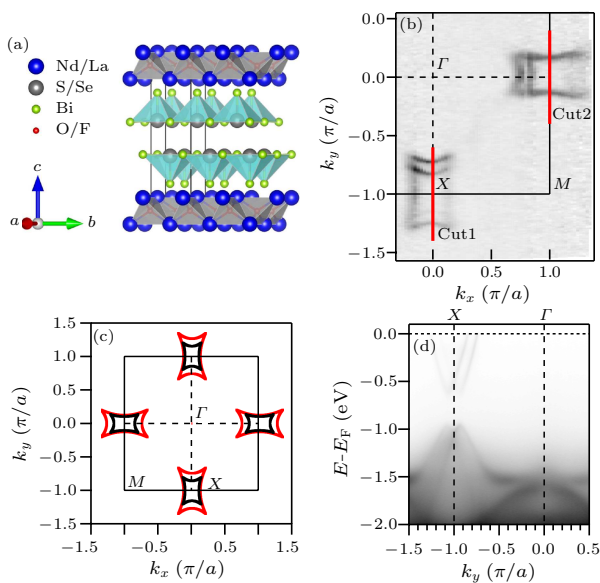


**Fig. 1.** (a) Representative crystal structure of  $\text{La}(\text{O},\text{F})\text{BiSe}_2$ . (b) ARPES intensity plot at  $E_F$  as a function of the two-dimensional wave vector taken at 22 K. The intensity is obtained by integrating the spectra within  $\pm 10$  meV with respect to  $E_F$ . Red lines labeled cuts 1 and 2 indicate the momentum locations, along which the data are shown in Figs. 2 and 3, respectively. The data were taken with 43 eV photons. (c) The schematic diagram of the two-dimensional Brillouin zone. (d) ARPES intensity plot along the high symmetry direction  $\Gamma$ - $X$  taken at 22 K.

Figure 1(a) shows the schematic diagram of the crystal structure, which is stacked by the  $\text{BiSe}_2$  bilayer and the  $\text{La}(\text{O}/\text{F})$  layers alternately. Previous ARPES results already revealed the rather two-dimensional character of this material by photon energy dependent experiments.<sup>[24,25]</sup> Figure 1(b) shows the FS mapping in the  $k_x$ - $k_y$  plane. We observe two FSs centered at

$X$ . The FSs exhibit significant separation along the  $\Gamma$ - $X$  direction, while almost degenerate along the  $M$ - $X$  direction. We plot the extracted FSs by assuming a fourfold symmetry with respect to  $\Gamma$  in Fig. 1(c). The two FSs enclose 8.2% and 3.3% of the Brillouin zone area, respectively. Counting the Luttinger volume of the two-dimensional FS sheets, the two observed FSs correspond to an electron doping of 0.23 per Bi site. Figure 1(d) shows the band dispersion along  $\Gamma$ - $X$  in an energy range within 2 eV below  $E_F$ . Several dispersive bands below  $-0.9$  eV and two electron-like band dispersion with a bottom around  $-0.6$  eV near  $X$  are observed here. The energy gap between them is around 0.3 eV, which is much smaller than the gap of  $\sim 0.9$  eV observed in the  $\text{BiS}_2$ -based system.<sup>[23]</sup>

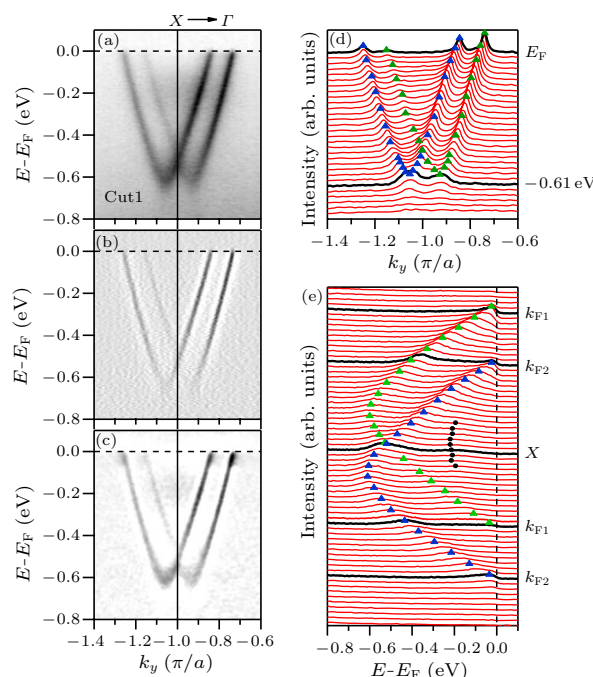


**Fig. 2.** (a) ARPES intensity plot along the  $\Gamma$ - $X$  direction (cut 1 from Fig. 1(b)) taken at 22 K. (b, c) The corresponding intensity plot of the second derivative along momentum and energy, respectively. (d) The corresponding MDCs. Blue and green triangles indicate the peak positions of the MDCs. (e) The corresponding EDCs. Blue and green triangles indicate the peak positions of the EDCs. Black curves represent the EDCs at  $k_{F1}$ ,  $k_{F2}$  and  $X$ . Here  $k_{F1}$  and  $k_{F2}$  are the Fermi wave vectors of the two electron-like bands. Black circles indicate the flat band.

To further examine the low-lying electronic band structure, we have carried out high precision ARPES measurements along  $\Gamma$ - $X$  (cut 1 in Fig. 1(b)) and  $M$ - $X$  (cut 2 in Fig. 1(b)), respectively. Figure 2(a) displays the ARPES intensity plot of the near- $E_F$  band dispersions along  $\Gamma$ - $X$ . Two discernible electron-like bands are observed along the  $\Gamma$ - $X$  direction, which is consistent with the LDA calculations.<sup>[29]</sup> The splitting magnitude of the electron-like bands is comparable with that in the  $\text{BiS}_2$ -based superconductors. Figures 2(b) and 2(c) display the corresponding intensity

plot of the second derivative along momentum and energy, respectively. Both bands are fast dispersing in energy and nearly have the same Fermi velocities along  $\Gamma$ - $X$ . By tracking the peaks in both the EDCs and MDCs, we resolved the band dispersion, which are indicated by blue and green triangles in Figs. 2(d) and 2(e). In addition to the electron-like bands, we observe a low-energy state characterized as a hump at  $-0.2$  eV in the EDCs in the vicinity of  $X$ , as marked with black circles in Fig. 2(e). Unlike the dispersive electron-like bands, this state is not predicted by the band calculations.

Figure 3(a) displays the ARPES intensity plot of the near- $E_F$  band dispersions along  $M$ - $X$ . The corresponding intensity plots of the second derivative along momentum and energy are displayed in Figs. 3(b) and 3(c), respectively. The band splitting along  $M$ - $X$  is discernible, though the splitting magnitude is much smaller than that along the  $\Gamma$ - $X$  direction. The splitting along  $M$ - $X$  has not been clearly resolved in the ARPES data reported previously.<sup>[24,25,30,31]</sup> Again, we observe the low-energy electronic state characterized as a hump at  $-0.2$  eV in the EDCs between the electron-like bands, as marked with black circles in Fig. 3(e). This state is more obviously seen in the data along  $M$ - $X$  than along  $\Gamma$ - $X$ , most likely related to the matrix element effects in the ARPES experiments. Although the peak position of the hump in the EDCs shifts slightly with momentum, this state does not exhibit observable dispersion in Figs. 3(a) and 3(c).

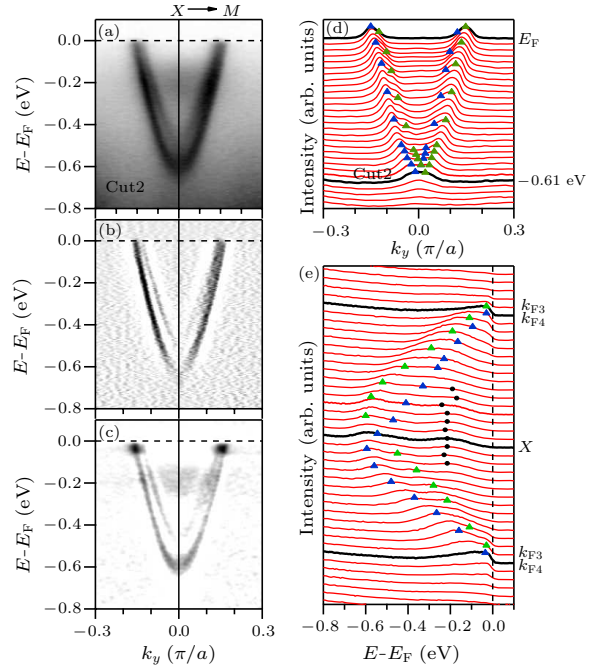


**Fig. 3.** (a) ARPES intensity plot along the  $M$ - $X$  direction (cut 2 from Fig. 1(b)) taken at 22 K. (b, c) The corresponding intensity plot of the second derivative along momentum and energy, respectively. (d) The corresponding MDCs. Blue and green triangles indicate the peak positions of the MDCs. (e) The corresponding EDCs. Black curves represent the EDCs at  $k_{F3}$ ,  $k_{F4}$  and  $X$ . Here  $k_{F3}$  and  $k_{F4}$  are the Fermi wave vectors of the two electron-like bands. Black circles indicate the non-dispersive band.

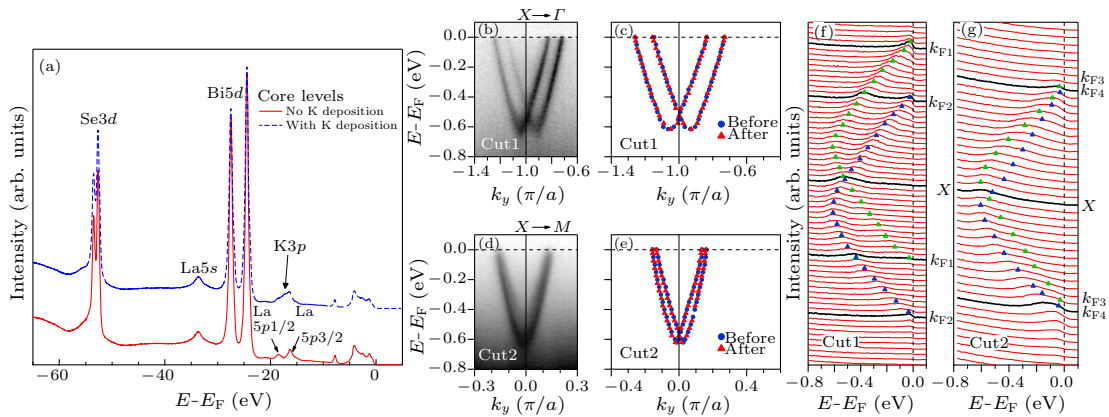


**Fig. 4.** (a) Core levels measured before (red) and after (blue) K evaporation, recorded with 100 eV photons. (b) ARPES intensity plot through the  $\Gamma$ - $X$  direction (cut 1 from Fig. 1(b)) taken at 22 K after 5 min K evaporation. (c) Extracted band dispersion of the electron-like bands before (blue) and after (red) K evaporation. (d, e) The corresponding intensity plot and extracted band dispersion along the  $M$ - $X$  direction (cut 2 from Fig. 1(b)). (f, g) The corresponding EDCs plots along  $\Gamma$ - $X$  and  $M$ - $X$  directions after K evaporation, respectively.

We further evaporate K atoms onto the cleaved surface. Figure 4(a) shows the core level spectra of the surface before and after K evaporation. Before K evaporation, we identify two peaks at binding energy  $E_B = 19.3$  and  $16.8$  eV, which are associated with La  $5p_{1/2}$  and  $5p_{3/2}$ , respectively. After K evaporation, these two peaks cannot be distinguished due to the

existence of the K  $3p$  core level at  $E_B \sim 18.3$  eV. The intensity plots along the two cuts  $\Gamma$ - $X$  and  $M$ - $X$  after K evaporation are shown in Figs. 4(b) and 4(d), respectively. We compare the extracted band dispersions along both directions before (blue) and after (red) K evaporation in Figs. 4(c) and 4(e). It turned out that there is no band shift after the K evaporation,

which means that no electrons are doped onto the surface via K evaporation. From the intensity plots we found that the non-dispersive band around  $X$  disappears after the K evaporation. This is further confirmed from the EDCs plots after evaporation shown in Figs. 4(f) and 4(g). We ascribe this non-dispersive band to the surface state because it is easily suppressed by K deposition. Surface state induced by polar surface has been observed in LaOFeAs with the same crystal structure as  $\text{LaO}_{0.5}\text{F}_{0.5}\text{BiSe}_2$ . For LaOFeAs, we observed a large Fermi surface induced by the polar surface.<sup>[32]</sup> However, we have not observed such a state in  $\text{La}(\text{O},\text{F})\text{BiSe}_2$ . Moreover, the LaOFeAs samples show a polarized cleaved surface that results from both  $[\text{LaO}]^{+1}$  and  $[\text{FeAs}]^{-1}$  surface termination layers. However, the cleaved plane for  $\text{La}(\text{O},\text{F})\text{BiSe}_2$  is between the two  $\text{BiSe}_2$  layers, which are weakly linked by the van der Waals force. Our argument can be further confirmed by an STM/STS study on  $\text{NdO}_{0.7}\text{F}_{0.3}\text{BiS}_2$  single crystals,<sup>[33]</sup> which demonstrated that the cleaving only occurred between the neighboring  $\text{BiS}_2$  layers and no evident surface segregation was observed. Based on the above facts, we obtain that the cleaved surface of  $\text{LaO}_{0.5}\text{F}_{0.5}\text{BiSe}_2$  is nonpolar without any charge redistribution, and the non-dispersive band should not be related to any polar surface. It might originate from the defects on the cleaved surface.

In summary, we have studied the electronic structure of  $\text{La}(\text{O},\text{F})\text{BiSe}_2$  single crystals with ARPES. We find two small electron-like FSs around  $X(\pi,0)$  instead of large FSs around  $\Gamma$  and  $M$  which are nested at the wave vector  $(\pi,\pi)$ , as proposed in recent theoretical models and one ARPES measurement. A non-dispersive band at around  $-0.2\text{ eV}$  is found along  $\Gamma-X$  and  $M-X$ , respectively. The K evaporation is performed to study the origin of the non-dispersive band, and the results suggest that this band might be related to the surface state caused by the defects on the cleaved surface. Our results provide detailed information on the low-energy electronic states and valuable insights for further experimental and theoretical studies of the pairing mechanism in  $\text{BiS}_2$ -based superconductors.

## References

- [1] Pickett W E 1989 *Rev. Mod. Phys.* **61** 433
- [2] Kamihara Y, Watanabe T, Hirano M and Hosono H 2008 *J. Am. Chem. Soc.* **130** 3296
- [3] Li S, Yang H, Fang D et al 2013 *Sci. Chin. Phys. Mech. Astron.* **56** 2019
- [4] Mizuguchi Y et al 2012 *Phys. Rev. B* **86** 220510
- [5] Singh S K, Kumar A, Gahtori B, Shruti, Sharma G, Patnaik S and Awana V P S 2012 *J. Am. Chem. Soc.* **134** 16504
- [6] Mizuguchi Y, Demura S, Deguchi K, Takano Y, Fujihisa H, Gotoh Y, Izawa H and Miura O 2012 *J. Phys. Soc. Jpn.* **81** 114725
- [7] S Demura et al 2013 *J. Phys. Soc. Jpn.* **82** 033708
- [8] Xing J, Li S, Ding X, Yang H and Wen H 2012 *Phys. Rev. B* **86** 214518
- [9] Jha R, Kumar A, S Kumar Singh and Awana V P S 2013 *J. Appl. Phys.* **113** 056102
- [10] Yazici D, Huang K, White B D, Chang A H, Friedman A J and Maple M B 2013 *Philos. Mag.* **93** 673
- [11] Yazici D et al 2013 *Phys. Rev. B* **87** 174512
- [12] Lin X et al 2013 *Phys. Rev. B* **87** 020504
- [13] Krzton-Maziopa A et al 2014 *J. Phys.: Condens. Matter* **26** 215702
- [14] Zhou T and Wang Z D 2013 *J. Supercond. Novel Magn.* **26** 2735
- [15] Li B, Xing Z W and Huang G Q 2013 *Europhys. Lett.* **101** 47002
- [16] Wan X, Ding C, Savrasov S Y and Duan G 2013 *Phys. Rev. B* **87** 115124
- [17] Yildirim T 2013 *Phys. Rev. B* **87** 020506
- [18] Martins G B, Moreo A and Dagotto E 2013 *Phys. Rev. B* **87** 081102
- [19] Awana V P S, Kumar A, Jha R, S Kumar Singh, Pal A, Shruti, Saha J and Patnaik S 2013 *Solid State Commun.* **157** 21
- [20] Usui H, Suzuki K and Kuroki K 2012 *Phys. Rev. B* **86** 220501
- [21] Xianxin W, Jing Y, Yi L, Heng F and Jiangping H 2014 *Europhys. Lett.* **108** 27006
- [22] Wu S F, Richard P, Wang X B, Lian C S, Nie S M, Wang J T, Wang N L and Ding H 2014 *Phys. Rev. B* **90** 054519
- [23] Zeng L K et al 2014 *Phys. Rev. B* **90** 054512
- [24] Xia M et al 2015 *J. Phys.: Condens. Matter* **27** 285502
- [25] Ye Z R et al 2014 *Phys. Rev. B* **90** 045116
- [26] Lee J et al 2013 *Phys. Rev. B* **87** 205134
- [27] Liu J Z et al 2014 *Europhys. Lett.* **106** 67002
- [28] Shao J F et al 2014 *Europhys. Lett.* **107** 37006
- [29] Feng Y, Ding C, Du Y, Wan X, Wang B, Savrasov S Y and Duan G 2014 *J. Appl. Phys.* **115** 233901
- [30] Sugimoto T et al 2015 *Phys. Rev. B* **92** 041113
- [31] Saini N L, Ootsuki D, Paris E, Joseph B, Barinov A, Tanaka M, Takano Y and Mizokawa T 2014 *Phys. Rev. B* **90** 214517
- [32] Zhang P et al 2016 *Phys. Rev. B* **94** 104517
- [33] Machida T, Fujisawa Y, Nagao M, Demura S, Deguchi K, Mizuguchi Y, Takano Y and Sakata H 2014 *J. Phys. Soc. Jpn.* **83** 113701